PERFORMANCE EVALUATION OF PERIPHERAL FINNED-TUBE EVAPORATORS BASED ON AN ENTROPY MINIMIZATION ANALYSIS

Bruno F Pussoli[1], pussoli@polo.ufsc.br
Jader R Barbosa Jr.[1], jrb@polo.ufsc.br
[1]POLO – Research Laboratories for Emerging Technologies in Cooling and Thermophysics - Federal University of Santa Catarina, 88040-900, Florianópolis, SC, Brazil.
Luciana W da Silva[2], Luciana_W_Silva@embraco.com.br
[2]Embraco. Av. Rui Barbosa 1020, 89219-901, Joinville, SC, Brazil
Massoud Kaviany[3], kaviany@umich.edu
[3]Department of Mechanical Engineering, University of Michigan, Ann Arbor, MI 48019, USA

Abstract. *This paper presents a second law-based performance assessment of a novel compact heat exchanger surface geometry for refrigeration applications. The so-called peripheral finned-tube evaporator is a cross-flow heat exchanger whose air-side is composed by a hexagonal arrangement of open-pore cells formed by radial fins whose bases are attached to the tubes and whose tips are connected to the peripheral fins. Each fin arrangement is made up of six radial fins and six peripheral fins forming a hexagon-like structure. The air-side fin configuration is composed of three levels of fin arrangement, each characterized by the length of radial fin and mounted with a 30^o offset from its neighboring level. A one-dimensional theoretical model based on the theory of porous media has been developed to predict the thermal-hydraulic behavior of the heat exchanger. The model incorporates the actual fin geometry into the calculation of the air-side porosity. The air-side permeability is calculated according to the Kozeny-Carman model with the particle diameter definition due to Whitaker. The determination of the overall dimensions of the peripheral finned-tube evaporator is based on a minimization of the entropy generation (due to fluid friction and heat transfer) on the air-side for a given air flow rate and refrigeration capacity.*

Keywords*: Peripheral finned-tube evaporator, compact heat exchangers, performance evaluation, entropy minimization*.

1. INTRODUCTION

Tube-fin heat exchangers are largely used as evaporators in household and light commercial refrigeration applications due to its low-cost, simple manufacture methods and availability of well-established methods and correlations for thermal-hydraulic (heat transfer and pressure drop) evaluation and sizing. Usually, the geometry of the evaporators used in "frost-free" appliances is such that the face area is smaller and the number of tube rows in the direction of the air flow is larger than in more conventional tube-fin heat exchanger geometries (Barbosa et al., 2009).

Automatic defrosting is an essential operation in "frost-free" appliances. The frost accumulated on the evaporator surfaces (fin and tubes) needs to be removed periodically so as to avoid obstruction of the air flow channels and is responsible for a deterioration of the evaporator thermal performance due to the combined effects of (i) increasing the conduction thermal resistance due low thermal conductivity of the frost layer and (ii) reducing the air flow rate due to the higher air-side pressure drop. Therefore, in order to account for the effect of frost build-up, "frost-free" evaporators cannot be made very compact (the typical fin pitch is of the order of 10 mm) which is undesirable from an appliance design point of view as precious space is taken by the evaporator inside the freezer compartment.

From a thermodynamic perspective, the current defrosting methods are particularly inefficient and fundamentally irreversible. Electric heaters are commonly utilized to eliminate the frost build-up on the heat exchanger surface, and the most usual types are aluminium sheathed coils mounted on the outer edge of the fins, parallel to the tubes. During normal operation, at pre-determined time intervals, the compressor is switched off and the heater is switched on in order to melt the frost accumulated on the evaporator. Thus, not only high grade energy (in the form of electricity) is dissipated as heat in the melting process, but this irreversible energy conversion takes place inside the refrigerator compartment, which represents an extra thermal load on the refrigeration system. Typical values of the defrost efficiency, defined as the ratio of the amount of energy required to melt the frost and the actual electrical energy dissipated as heat during the defrost mode, are of the order of 5-15%. Therefore, new approaches are needed — both in terms of defrost strategy and frost-robustness of the components — in order to minimize the thermodynamic performance penalty associated with the frost management in household and light commercial refrigeration appliances.

Recently, Kaviany and co-workers (Kaviany, 2006; Wu et al., 2007) put forward an alternative air-side heat exchanger geometry intended for enhanced thermal performance under dehumidifying conditions in comparison with conventional plain fin-tube evaporators. As such, the proposed geometry allows for uninterrupted and effective air flow even on the presence of condensate and frost. The so-called peripheral finned-tube evaporator (see Fig. 1) is a cross-flow heat exchanger whose air-side is composed by a hexagonal arrangement of open-pore cells formed by radial fins whose bases are attached to the tubes and whose tips are connected to the peripheral fins. Each fin arrangement is made

up of six radial fins and six peripheral fins forming a hexagon-like structure. The air-side fin configuration is composed of three levels of fin arrangement, each characterized by the length of radial fin and mounted with a 30^o offset from its neighboring level. Wu et al. (2007) advanced a model for the heat transfer in the radial and peripheral fins in the fin arrangement. CFD simulations were also carried out to investigate the local structure of the fluid flow field in the heat exchanger matrix both with and without frost build-up in the vicinity of the tubes. They identified that, as the conduction heat transfer through the radial fins is the main path for heat flow to the tubes, frost blockage surrounding the tube does not deteriorate the thermal-hydraulic performance significantly.

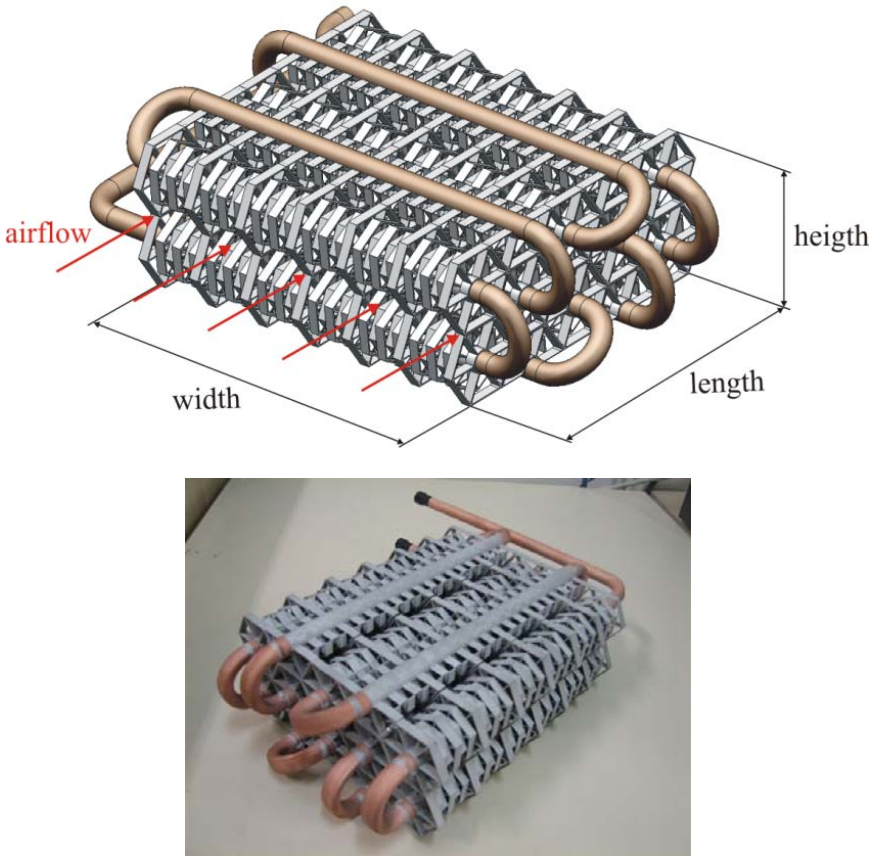

Figure 1. Peripheral fin heat exchanger.

The optimum geometric configuration of a given heat exchanger can be achieved in a number of ways which depend on the level of detail with which the parameters of the thermal system where the heat exchanger is included are accounted for in the objective function and associated constraints (Pira et al., 2000). Thus, an optimum evaporator configuration which is obtained based only on the maximization of the ratio of the cooling capacity and the fan pumping power may not be the desired configuration on the system level, i.e., the one that provides the highest system COP (Waltrich, 2008).

Shah and Sekulic (2003) and Webb and Kim (2005) present a general overview of performance evaluation criteria (PEC) for heat transfer surfaces and heat exchangers with and without phase change. Yilmaz and co-workers (Yilmaz et al., 2001; 2005) reviewed the existing first-law and second-law based PEC. Basically, second-law-based PEC are formulated so as to achieve a minimum entropy generation (or a minimum exergy destruction) in a particular application. Bejan (1982, 1996) demonstrated the use of entropy generation minimization (EGM) for optimization of different devices and systems, including heat exchangers. Hesselgreaves (2000) reviewed several second-law-based approaches of PEC and presented a rational calculation method by deriving new relations for the local rate generation process and for the nearly-balanced counterflow arrangement. Zimparov (2000) developed extended PEC equations for enhanced heat transfer surfaces based on the entropy production theorem so as to include the effect of fluid temperature variation along the length of a tubular heat exchanger. Khan and Yovanovich (2007) applied the EGM method to study the thermodynamic losses caused by heat transfer and pressure drop in the air flow in a cylindrical pin-fin heat sink considering the effect of flow by-pass.

This is the first communication of a joint research effort by the Federal University of Santa Catarina, the University of Michigan and Embraco to study the fundamentals and the design aspects of peripheral fin heat exchangers. The objectives of the present paper are (i) to put forward a one-dimensional calculation procedure of the air-side thermal

conductance and pressure drop, and (ii) to present a preliminary EGM based performance evaluation of the peripheral fin evaporator under dry conditions. The one-dimensional model of the heat transfer at the level of the fin arrangement proposed by Wu et al. (2007) was incorporated into the calculation procedure. Closure relationships for the friction factor and heat transfer coefficients derived from the theory of porous media (Kaviany, 1995) have been utilized. As will be seen, the thermal-hydraulic performance of the peripheral fin heat exchanger under typical laboratory test conditions is such that it provides roughly the same heat transfer rate and the same thermal conductance as conventional tube-fin "no-frost" evaporators with approximately 22% of the surface area. However, the calculated pressure drop is significantly higher than those encountered in less compact tube-fin geometries.

2. MODELING

2.1. Heat transfer in the fin arrangement

The heat transfer in the fin arrangement was investigated by Wu et al., (2007) and only the main features of their model will be described here. The geometry of a typical fin arrangement consisting of six radial fins and six peripheral fins is shown in Fig. 2. The kernel of the model is a thermal equilibrium condition at the junction between each radial fin and two peripheral fins given by:

$$Q_{r,tip} = 2Q_{p,b} \tag{1}$$

where Q is the heat transfer rate and the subscripts b, p, r and tip stand for fin base, peripheral fin, radial fin and fin tip, respectively. Equation (1) is solved for the excess temperature of the radial fin tip, θ_{tip}. By assuming symmetry with respect to the mid-plane of the peripheral fin, one has:

$$Q_{p,b} = \theta_{tip}\left(\frac{P_p k_s A_{k,p}}{A_p R_p}\right)^{1/2} \tanh\left[\left(\frac{P_p}{k_s A_{k,p} A_p R_p}\right)^{1/2} L_p\right] \tag{2}$$

where P_p is the peripheral fin perimeter, L_p is the peripheral fin length, $A_{k,p}$ is the cross-sectional area, A_p is the surface area, k_s is the thermal conductivity of the (solid) fin and R_p is the convection heat transfer resistance associated with the peripheral fin.

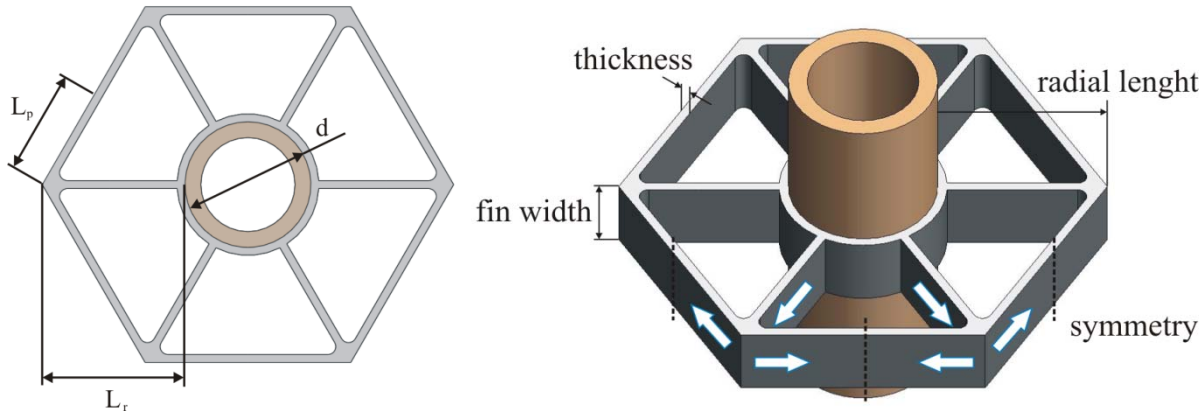

Figure 2. Adiabatic tip condition of a mid-plane on a peripheral fin.

The heat transfer rate in the radial fin is given by:

$$Q_{r,tip} = -k_s A_{k,r} \left.\frac{d\theta_r}{dx}\right|_{x=L_r} \tag{3}$$

By assuming prescribed excess temperatures at the radial fin base and at the radial fin tip, one has:

$$\frac{\theta_r(x)}{\theta_b} = \frac{(\theta_{tip}/\theta_b)\sinh\left[\left(\frac{P_r}{k_s A_{k,r} A_r R_r}\right)^{1/2} x\right] + \sinh\left[\left(\frac{P_r}{k_s A_{k,r} A_r R_r}\right)^{1/2} (L_r - x)\right]}{\sinh\left[\left(\frac{P_r}{k_s A_{k,r} A_r R_r}\right)^{1/2} (m_r L_r)\right]} \tag{4}$$

where P_r is the radial fin perimeter, L_r is the radial fin length, $A_{k,r}$ is the cross-sectional area, A_r is the surface area and R_r is the convection heat transfer resistance associated with the radial fin. By substituting the first derivative of Eq. (4) at $x = L_r$ into Eq. (1), the excess temperature that satisfies the equilibrium condition is found and the temperature profiles in the radial and peripheral fins are determined. The convection heat transfer resistances in the radial and peripheral fins are defined as:

$$R_{r(p)} = \frac{D_p}{A_{r(p)} Nu_{Dp} k_f} \frac{\varepsilon}{(1-\varepsilon)} \tag{5}$$

where ε is the heat exchanger porosity defined as the fraction of the total volume occupied by air. D_p is the equivalent particle diameter defined as the ratio of six times the solid volume and the interstitial area. k_f is the thermal conductivity of the fluid and Nu_{Dp} is the Nusselt number for porous media interstitial surface area calculated according to the Whitaker correlation (Kaviany, 1995):

$$Nu_{Dp} = 2 + (0.4 Re_{Dp}^{0.5} + 0.2 Re_{Dp}^{\frac{2}{3}}) Pr^{0.4} \tag{6}$$

where Pr is the Prandtl number and Re_{Dp} is the particle Reynolds number given by:

$$Re_{Dp} = \frac{U_f D_p}{\nu_f (1-\varepsilon)} \tag{7}$$

where U_f is the velocity of the fluid upstream of the heat exchanger and ν_f is the fluid kinematic viscosity.

2.2. Heat exchanger model

The heat exchanger model consists of dividing the heat exchanger into one-dimensional control volumes of length L in the direction of the flow (see Fig. 3) and of applying energy and momentum balances in each control volume. The face velocity, the face area, the inlet pressure and the inlet temperature are known. The temperature of the tube wall, T_b, is assumed constant over the whole length of the heat exchanger (i.e., as in an evaporator with negligible refrigerant pressure drop and vapor superheating). For each control volume, the heat transfer rate and the outlet temperature are calculated according to the following heat balance (assuming a pure counterflow configuration):

$$\dot{m}_f c_{p,f} \left(T_{out,CV} - T_{in,CV}\right) = \eta_0 \bar{h} A_{CV} \Delta T_{lm} \tag{8}$$

where $\dot{m}_f$ is the mass flow rate, $c_{p,f}$ is the specific heat capacity of the fluid and $T_{in,CV}$ and $T_{out,CV}$ are the bulk fluid temperature entering and leaving the control volume. A_{CV} is the interstitial area in the control volume. ΔT_{lm} is the logarithmic mean temperature difference given by:

$$\Delta T_{lm} = \frac{(T_{out,CV} - T_{in,CV})}{ln\left(\frac{T_b - T_{in,CV}}{T_b - T_{out,CV}}\right)} \tag{9}$$

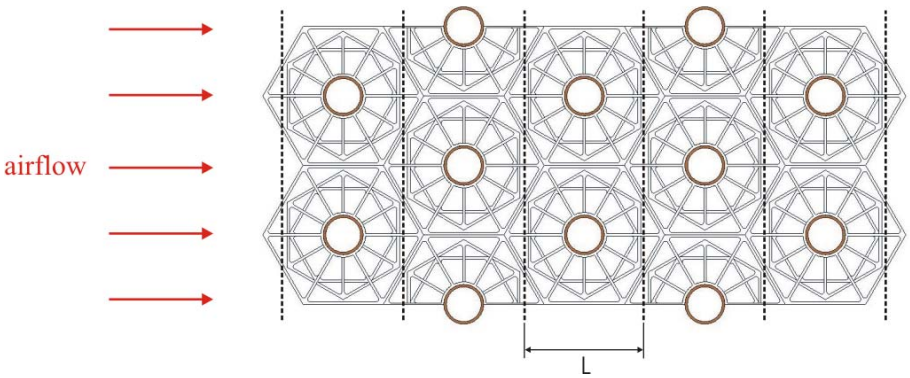

Figure 3. Peripheral fin heat exchanger separated in control volumes.

As mentioned above, the extended surface is composed of three distinct levels of fin arrangement, each characterized by a specific radial fin length, as seen in Fig. 1. Thus, the overall surface efficiency is calculated based on

the number of fin arrangements of a particular size (N_1, N_2 and N_3) and on the corresponding surface area of each individual arrangement (A_1, A_2 and A_3) as follows:

$$\eta_0 = \frac{N_1\eta_1A_1+N_2\eta_2A_2+N_3\eta_3A_3}{N_1A_1+N_2A_2+N_3A_3} \tag{10}$$

where η_1, η_2 and η_3 are the fin efficiencies of each fin arrangement given by:

$$\eta_i = \frac{\left(6Q_{r,b}+Q_{bare}\right)_i}{\left(Q_{maximum}\right)_i} \tag{11}$$

where:

$$Q_{bare} = \bar{h}A_{bare}(T_b - \bar{T}_{CV}) \tag{12}$$

$$Q_{r,b} = -k_sA_{k,r}\left.\frac{d\theta_r}{dx}\right|_{x=0} \tag{13}$$

$$Q_{maximum} = \bar{h}A(T_b - \bar{T}_{CV}) \tag{14}$$

In the above equations A_{bare} is the area of the tube exposed to the fluid flow and A is the interstitial area of each fin arrangement. $\bar{T}_{CV}$ is the average bulk fluid temperature in the control volume, calculated as the arithmetic average between the inlet and outlet temperatures. The average heat transfer coefficient is calculated as follows (Kaviany, 1995):

$$\bar{h} = k_f\frac{Nu_{Dp}}{D_p}\frac{(1-\varepsilon)}{\varepsilon} \tag{15}$$

The air-side pressure drop is calculated according to a classical Kozeny-Carman formulation as follows (Kaviany, 1995; Holdich, 2003):

$$\frac{\Delta P}{L} = f\frac{6(1-\varepsilon)\rho U_f^2}{D_p\,\varepsilon^3} \tag{16}$$

where S_v is the specific surface area per unit of solid volume ($S_v = 6/D_p$) and f is the Carman friction factor whose dependency on the Reynolds number is given by the following relationship:

$$f = \frac{5}{\left(\frac{Re_{Dp}}{6}\right)} + \frac{0.4}{\left(\frac{Re_{Dp}}{6}\right)^{0.6}} \tag{17}$$

2.3. Entropy generation minimization

In this section, a relationship for the rate of entropy generation in internal flows (Bejan, 1982; 1996) is coupled with the present formulation in order to determine the optimum length of the peripheral fin heat exchanger for a particular application subjected to a number of constraints. After a combination of energy and entropy balances in an increment *dx* in the flow direction, the entropy generation rate per unit length in a duct of arbitrary geometry is given by:

$$\dot{S}'_{gen} = \frac{q'\Delta T}{T^2} + \frac{\dot{m}}{\rho T}\left(-\frac{dP}{dx}\right) \tag{18}$$

where q' is the heat transfer rate per unit length and ΔT is the difference between the wall temperature and the bulk fluid temperature. In order to calculate the overall entropy generation rate, the above equation has to be integrated along the heat exchanger. In the present paper, the total entropy generation rate was calculated as follows:

$$\dot{S}_{gen} = \sum_{i=1}^{n}\dot{S}_{gen,CV} \tag{19}$$

where n is the number of tube rows (or control volumes) and $\dot{S}_{gen,CV}$ is the rate of entropy generation in each control volume, given by:

$$\dot{S}_{gen.CV} = \frac{q'_{CV}\Delta T_{CV}}{T_{CV}^2} + \frac{\dot{m}}{\rho T_{CV}}(-\Delta P_{CV}) \tag{20}$$

where the subscripts *CV* refer to the local property of the control volume. The entropy generation number is the dimensionless entropy generation rate given by:

$$N_s = \frac{\dot{S}_{gen}}{\dot{m}c_{p,f}} \tag{21}$$

3. RESULTS AND DISCUSSION

The model equations were implemented in the Engineering Equation Solver (EES) (Klein, 2009) in order to obtain the temperature and pressure profiles along the heat exchanger and the heat transfer rate. The proposed geometry and operating conditions are representative of those which will be evaluated experimentally in a wind-tunnel calorimeter especially designed for evaluating the thermal-hydraulic performance of "no-frost" evaporators under dry conditions (i.e., no dehumidification). Therefore, in the present calculations, air is the external fluid (inlet temperature of 20°C) with volumetric flow rates ranging from 5 to 30 L/s. The fins are made of aluminum and the wall (fin base) temperature is assumed constant and uniform (40°C). The air properties are evaluated locally at each control volume and the properties of the fin are evaluated at the base temperature. The heat exchanger dimensions (see Fig. 1) are as follows: 55.56 mm (height), 124.0 mm (width) and 80.34 mm (length), which corresponds to 3 tube rows in the flow direction (notice that the heat exchanger in Figs. 1 and 3 has 5 tube rows). The surface area is 0.2145 m^2. The dimensions of the fin arrangements (levels 1, 2 and 3) are summarized in Table 1. In the present study, the fin levels are arranged in the following order: L3-L2-L1-L2-L1-L2-L3 (Wu et al., 2007).

Table 1. Geometric dimensions of the peripheral fin heat exchanger (in mm)

radial length - L_{r3}	radial length - L_{r2}	radial length - L_{r1}	thickness	fin width	tube diameter - d
12.1	9.0	7.0	0.5	4.0	7.94

The behavior of the calculated heat transfer rate, pressure drop and air-side thermal conductance (calculated as the ratio of the heat transfer rate and the logarithmic mean temperature difference) as a function of the air flow are shown in Figs. 5, 6 and 7, respectively. In comparison with conventional tube-fin "no-frost" evaporators operating under the same conditions (temperatures and flow rate), the peripheral fin heat exchanger gives roughly the same air-side thermal conductance with approximately 22% of the overall surface area (see Barbosa *et al.*, 2009). However, this advantage of being more compact comes at the expense of a larger pressure drop and, consequently, a higher pumping power. Experimental campaigns are currently being prepared at the Federal University of Santa Catarina to determine the air-side thermal conductance and pressure drop characteristics of peripheral fin evaporator prototypes, such as the one shown in Fig. 1.

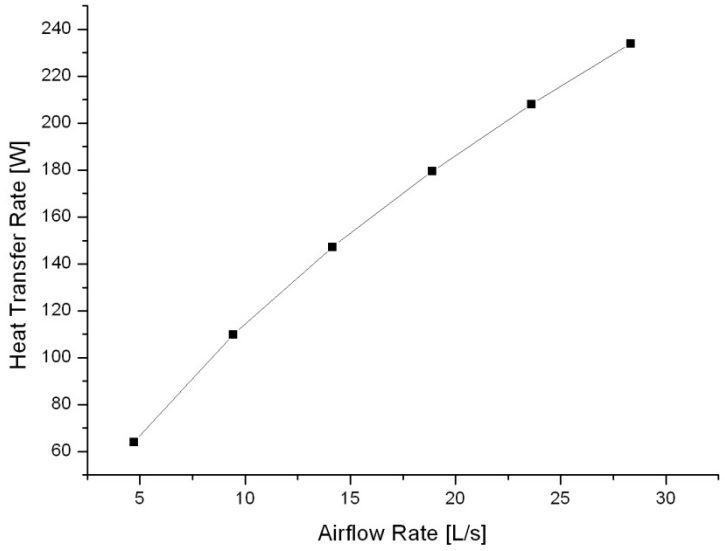

Figure 5. Heat transfer rate as a function of the air flow rate for a fixed heat exchanger geometry.

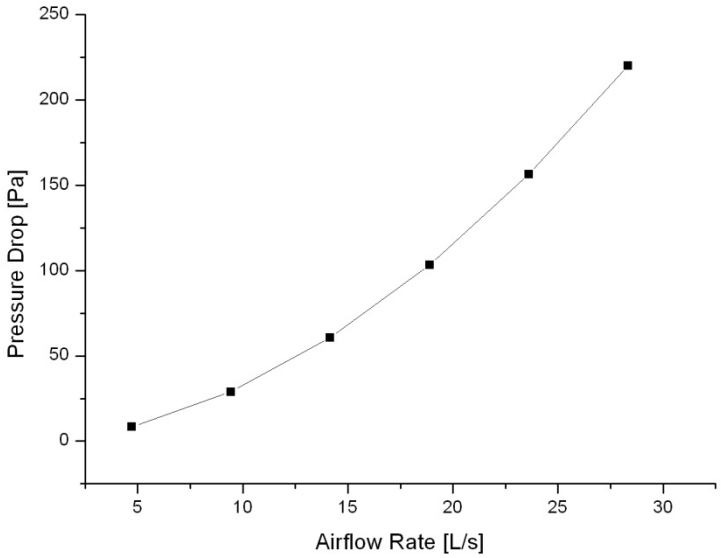

Figure 6. Air-side pressure drop.

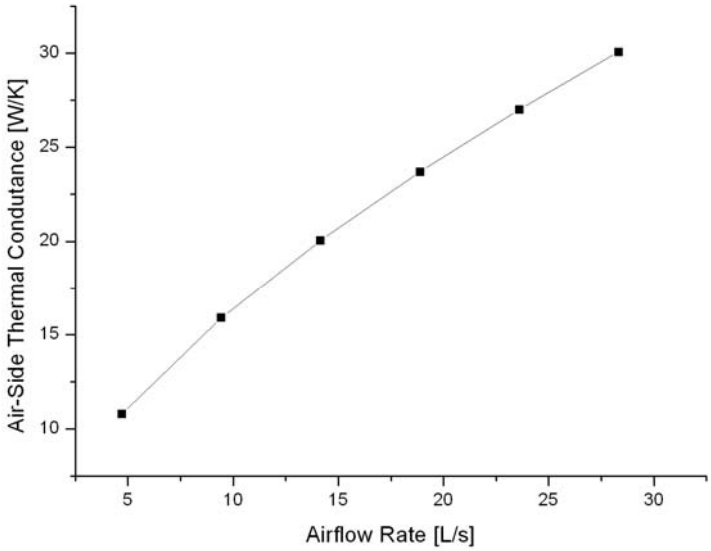

Figure 7. Air-side thermal conductance.

In order to illustrate the use of EGM in the optimization of the peripheral fin heat exchanger, a simple analysis was conducted in which two operational parameters (the heat transfer rate and the air flow rate) were fixed at the design values of 300 W and 19 L/s, respectively. The face area of the heat exchanger (55.56 × 124.0 mm) and the dimensions of the fin arrangements (see Table 1) were also kept constant. Thus, by varying the number of tube rows, it is possible to obtain a specific heat exchanger length that minimizes the entropy generation rate in the heat exchanger. Figure 8 illustrates the behavior of the entropy generation number (eq. 21) as a function of the number of tube rows. For small values of number of tube rows, the heat transfer part of the entropy generation number dominates because of the large difference between the wall temperature and the bulk temperature and the small surface area (which results in a large heat transfer rate per unit length). The behavior of the difference between the wall temperature and the inlet bulk fluid temperature is illustrated in Fig. 9. Also, with fewer tube rows, the fluid friction contribution to the entropy generation is minimal. On the other hand, for large values of number of tube rows, the heat transfer contribution decreases significantly as the surface area increases and the wall temperature difference decreases. Conversely, the fluid friction contribution dominates as the pressure drop is directly influenced by the number of tube rows. As can be seen from Fig. 8, the optimum number of tube rows for the conditions specified above is around seven. Naturally, the analysis needs to be developed further in order to take into account different scenarios (in terms of conditions and constraints) and the

presence of frost and/or condensate formation so as to develop a more comprehensive performance evaluation of peripheral fin heat exchanger.

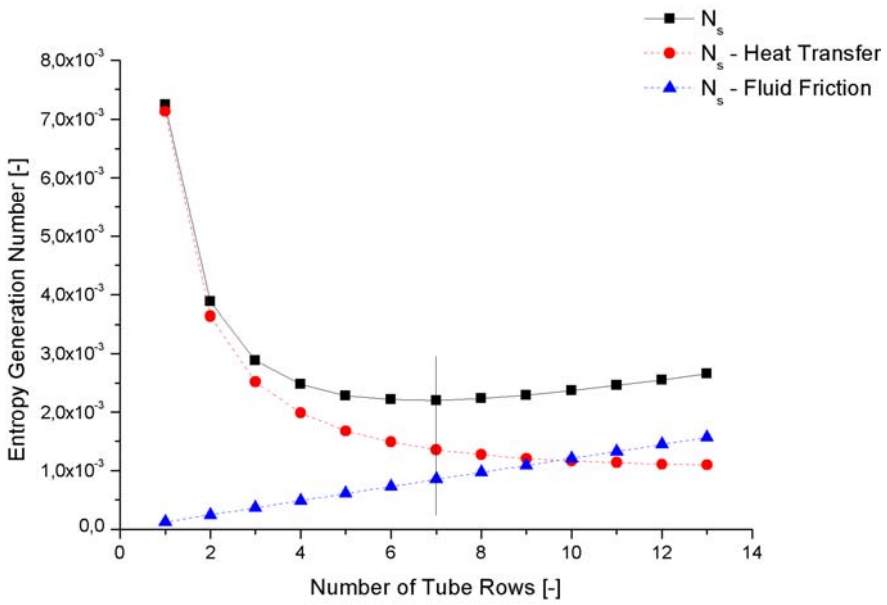

Figure 8. Behavior of the entropy generation number as a function of the number of tube rows for fixed heat transfer capacity and air flow rate.

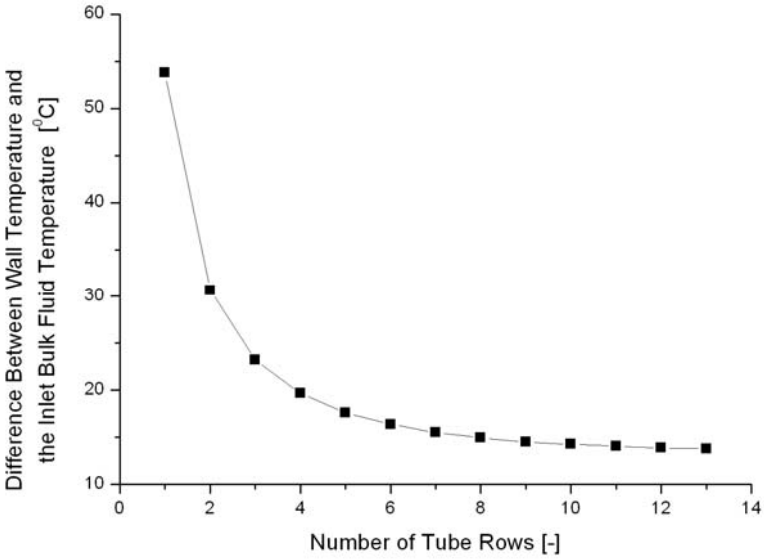

Figure 9. Difference between the wall temperature and the inlet bulk fluid temperature as a function of the number of tube rows for fixed heat transfer capacity and air flow rate.

4. CONCLUSIONS

This paper presented a theoretical evaluation of the thermal-hydraulic performance of the peripheral fin heat exchanger (Kaviany, 2006; Wu et al., 2007). The one-dimensional heat transfer analysis at the fin arrangement level (Wu et al., 2007) was incorporated into an overall heat exchanger calculation in order to predict the heat transfer rate, the pressure drop and the overall thermal conductance. The heat exchanger model is based on the theory of porous media and incorporates the actual fin geometry and the fin temperature profiles into the calculation of the air-side porosity and of the overall surface efficiency, respectively. The air-side permeability is calculated according to the Kozeny-Carman model with the particle diameter definition due to Whitaker. The model was further combined with and

EGM based performance evaluation in order to determine the optimum heat transfer configuration for a specific application. Overall, the results showed some general consistency with the expected trends and expected performance of the peripheral fin heat exchanger in a qualitative comparison with conventional tube-fin "no-frost" evaporators operating under similar conditions. Evidently, experimental data are needed to validate the model so that the performance evaluation can be extended to a number of different scenarios. The experimental tests are currently being performed and shall be reported in the future.

5. ACKNOWLEDGEMENTS

This work is part of a long-standing technical-scientific cooperation between the Federal University of Santa Catarina and Embraco. Financial support from FINEP and CNPq (under the National Institutes of Science and Technology program) is duly acknowledged.

6. REFERENCES

Barbosa, Jr., J.R., Melo, C., Hermes, C.J.L., Waltrich, P.J., 2009, "A study of the air-side heat transfer and pressure drop characteristics of tube-fin 'no-frost' evaporators", Appl. Energy, Vol. 86, No. 9, pp. 1484-1491.

Bejan, A., 1982, "Entropy generation through heat and fluid flow". Wiley, New York.

Bejan, A., 1996, "Entropy generation minimization: The new thermodynamics of finite-size devices and finite-time processes", Appl. Phys. Rev., Vol. 79, No. 3, pp. 1191-1218.

Hesselgreaves J.E., 2000, "Rationalization of second law analysis of heat exchangers", Int. J. Heat Mass Transfer 43, pp. 4189–4204.

Holdich R.G., 2003, "Fundamentals of Particle Technology", Midland Information Technology and Publishing, http://www.midlandit.co.uk.

Kaviany M., 1995, "Principles of heat transfer in porous media", 2nd ed., Springer, New York.

Kaviany M., 2006, "Robust heat exchanger under condensate and frosting conditions", Provisional patent application, UMJ-184-A (UM 3251).

Khan W.A. Yovanovich M.M., 2007, "Optimization of pin-fin heat sinks in bypass flow using entropy generation minimization method", Proceedings of IPACK2007, ASME InterPACK '07, Vancouver, BC, Canada, Paper IPACK2007-33983

Klein, S. A., 2009, Engineering Equation Solver (EES), F-Chart Software, Professional Version 8.328-3D.

Pira, J.V., Bullard, C.W., Jacobi, A.M., 2000, "An evaluation of heat exchangers using system information and PEC", Air Conditioning and Refrigeration Center, ACRC Report TR-175, University of Illinois, Urbana.

Shah, R. K., Sekulic, D. P., 2003, "Fundamentals of Heat Exchanger Design", John Wiley and Sons, New York, USA.

Waltrich, P. J., 2008, "Análise e otimização de evaporadores de fluxo acelerado aplicados a refrigeração doméstica", M. Eng. dissertation, Universidade Federal de Santa Catarina, Florianópolis, SC, Brasil.

Webb, R. L., Kim, N-H. 2005, "Principles of Enhanced Heat Transfer", 2nd ed., Taylor & Francis, New York.

Wu H., Ma D., Kaviany M., 2007, "Peripheral fins for blockage robustness", Int. J. Heat Mass Transfer Vol. 50, pp.2514-2520.

Yılmaz M., Karslı S., and Sara, O.N., 2001, "Performance evaluation criteria for heat exchangers based on second law analysis", Exergy Int., Vol. 1, No. 4, pp. 278–294.

Yılmaz M., Comakli O., Yapici S., Sara O.N., 2005, "Performance evaluation criteria for heat exchangers based on first law analysis", J. Enhanced Heat Transfer, Vol. 12, No. 2, pp. 121–157.

Zimparov, V.D., 2001, "Extended performance evaluation criteria for enhanced heat transfer surfaces: heat transfer through ducts with constant heat flux", Int. J. Heat Mass Transfer, Vol. 44, No. 1, pp. 169-180.

7. RESPONSIBILITY NOTICE

The authors are the only responsible for the printed material included in this paper.